

# Deletion of *Nedd4-2* results in progressive kidney disease in mice

Tanya L Henshall<sup>1,4</sup>, Jantina A Manning<sup>1,4</sup>, Omri S Alfassy<sup>1,4</sup>, Pranay Goel<sup>1,2,4</sup>, Natasha A Boase<sup>1</sup>, Hiroshi Kawabe<sup>3</sup> and Sharad Kumar<sup>\*,1,2</sup>

**NEDD4-2 (NEDD4L), a ubiquitin protein ligase of the Nedd4 family, is a key regulator of cell surface expression and activity of the amiloride-sensitive epithelial Na<sup>+</sup> channel (ENaC). While hypomorphic alleles of *Nedd4-2* in mice show salt-sensitive hypertension, complete knockout results in pulmonary distress and perinatal lethality due to increased cell surface levels of ENaC. We now show that *Nedd4-2* deficiency in mice also results in an unexpected progressive kidney injury phenotype associated with elevated ENaC and Na<sup>+</sup>Cl<sup>-</sup> cotransporter expression, increased Na<sup>+</sup> reabsorption, hypertension and markedly reduced levels of aldosterone. The observed nephropathy is characterized by fibrosis, tubule epithelial cell apoptosis, dilated/cystic tubules, elevated expression of kidney injury markers and immune cell infiltration, characteristics reminiscent of human chronic kidney disease. Importantly, we demonstrate that the extent of kidney injury can be partially therapeutically ameliorated in mice with nephron-specific deletions of *Nedd4-2* by blocking ENaC with amiloride. These results suggest that increased Na<sup>+</sup> reabsorption via ENaC causes kidney injury and establish a novel role of NEDD4-2 in preventing Na<sup>+</sup>-induced nephropathy. Contrary to some recent reports, our data also indicate that ENaC is the primary *in vivo* target of NEDD4-2 and that *Nedd4-2* deletion is associated with hypertension on a normal Na<sup>+</sup> diet. These findings provide further insight into the critical function of NEDD4-2 in renal pathophysiology.**

*Cell Death and Differentiation* (2017) 24, 2150–2160; doi:10.1038/cdd.2017.137; published online 1 September 2017

Na<sup>+</sup> homeostasis in the kidney is critical for the maintenance of blood volume and blood pressure (BP). The Na<sup>+</sup> reabsorption in the nephron is mediated via the Na<sup>+</sup>Cl<sup>-</sup> co-transporter (NCC) in the distal convoluted tubule (DCT), and through the amiloride-sensitive epithelial Na<sup>+</sup> channel (ENaC) in the connecting tubule (CNT), distal tubule (DCT) and the collecting duct (CD). Both NCC and ENaC are regulated by the ubiquitin protein ligase, NEDD4-2.<sup>1–5</sup> Although NEDD4-2 is known to ubiquitinate and regulate the expression of many cell surface proteins, the most studied targets of NEDD4-2 are the three subunits ( $\alpha$ ,  $\beta$  and  $\gamma$ ) of ENaC. The WW domains of NEDD4-2 have been demonstrated to directly bind to the PPXY motifs present in the cytoplasmic C termini of all three ENaC subunits leading to their ubiquitination, endocytosis and degradation.<sup>2,3</sup> Thus, an expected consequence of the loss of *Nedd4-2* is increased cell surface expression and membrane retention of ENaC, resulting in increased ENaC activity.<sup>1</sup> The significance of NEDD4-2-dependent regulation of ENaC in the maintenance of Na<sup>+</sup> homeostasis is apparent from Liddle's syndrome, characterized by constitutively elevated ENaC activity and hypertension due to mutations in the PY motifs of  $\beta$ - and  $\gamma$ -ENaC, which abrogate the interaction between ENaC and NEDD4-2.<sup>2</sup>

NEDD4-2 is widely expressed during mouse development and in adult tissues, with particularly high expression in the liver, kidney, heart, brain and lung.<sup>1,6</sup> The studies of *Nedd4-2* knockout (KO) mice have provided useful and also somewhat unexpected and contradictory insights into the *in vivo* function

of NEDD4-2. A *Nedd4-2* KO mouse line (*Nedd4-2*  $\Delta$  exons 6–8, which includes an alternative translation start site and WW domain 1) express small amounts of *Nedd4-2* splicing isoforms.<sup>7</sup> These mice appear normal but show slightly increased ENaC expression and hypertension upon feeding a high-salt diet.<sup>7</sup> A renal-tubule-specific *Nedd4-2* conditional KO mouse with the same mutation (*Nedd4L*<sup>Pax8/LC1</sup>) demonstrated that hypertension is largely due to increased expression and activity of the NCC.<sup>8</sup> Recently, it was shown that  $\alpha$  and  $\gamma$  (but not  $\beta$ ) ENaC levels are increased when these mice are fed a long-term, low K<sup>+</sup> diet.<sup>9</sup>

A KO line generated in our laboratory in which all *Nedd4-2* splicing variants are absent (*Nedd4-2*  $\Delta$  exons 15–16) display increased ENaC expression in the lung and kidney, with perinatal death of animals due to respiratory distress as a result of failure of lungs to inflate, or severe sterile inflammation of the lung.<sup>5</sup> The different severity of the phenotypes between these lines is likely due to the hypomorphic nature of the *Nedd4-2*  $\Delta$  exons 6–8 allele. This is supported by studies with another independent line where *Nedd4-2* KO results in perinatal death,<sup>10</sup> and a conditional KO of *Nedd4-2* in the lung that was found to be sufficient for animals to develop inflammatory lung disease, leading to perinatal lethality.<sup>10</sup>

To determine the effect of *Nedd4-2* loss in the kidney, we analyzed the pathology of *Nedd4-2*  $\Delta$  exons 15–16 mice. We report here that *Nedd4-2* loss results in progressive kidney damage beginning immediately after birth. Additionally, we confirm this pathology in a kidney tubule-specific *Nedd4-2* KO

<sup>1</sup>Centre for Cancer Biology, University of South Australia and SA Pathology, Adelaide, SA 5000, Australia; <sup>2</sup>School of Medicine, University of Adelaide, Adelaide, SA 5005, Australia and <sup>3</sup>Max Planck Institute of Experimental Medicine, Department of Molecular Neurobiology, Göttingen 37075, Germany

\*Corresponding author: S Kumar, Centre for Cancer Biology, University of South Australia and SA Pathology, Frome Road, PO Box 14, Rundle Mall, Adelaide, SA 5000, Australia. Tel: +61 8 8222 3738; Fax: +61 8 8222 3139; E-mail Sharad.Kumar@unisa.edu.au

<sup>4</sup>These authors contributed equally to this work.

Received 07.6.17; revised 05.7.17; accepted 19.7.17; Edited by G Melino; published online 01.9.17

mouse line, *Nedd4-2<sup>Ksp1.3</sup>*. We further show that increased ENaC activity contributes to the observed kidney damage.

We therefore provide the first evidence that loss of *Nedd4-2* results in early and progressive kidney damage. Given our demonstration of a direct and critical role for ENaC in renal injury, our *Nedd4-2* KO mice can be a valuable resource for the study of the effects of salt on progression of kidney damage.

## Results

***Nedd4-2<sup>-/-</sup>* kidney pathology consistent with kidney damage.** We have previously described a perinatal lethal phenotype of *Nedd4-2<sup>-/-</sup>* mice due to respiratory distress; however, a small percentage of animals survive up to 3 weeks of age.<sup>5</sup> To determine the role of NEDD4-2 in the kidney, we carried out pathological analysis of kidneys from wild-type and surviving *Nedd4-2<sup>-/-</sup>* mice at postnatal (P) day 20. Kidneys from *Nedd4-2<sup>-/-</sup>* mice appeared pale and showed histological changes consistent with renal damage, including a disorganized structure and numerous cortical cysts with necrotic cellular debris, often with luminal stenosis/obstruction (Figure 1a). Large areas of mesenchyme were observed by histology, immunohistochemistry and real-time quantitative PCR (qRT-PCR) for the mesenchymal marker, vimentin (Figures 1b and c). In addition, *Nedd4-2<sup>-/-</sup>* kidneys showed obvious fibrotic damage occupying a large portion of the cortex revealed by immunohistochemistry and qRT-PCR for  $\alpha$ -1 type 1 collagen. Consistent with kidney injury, expression of the myofibroblast marker,  $\alpha$ -smooth muscle actin (SMA), and marker for proximal tubule kidney injury, kidney injury molecule-1 (KIM-1, also referred to as T-cell immunoglobulin mucin (TIM-1)),<sup>11</sup> was upregulated in *Nedd4-2<sup>-/-</sup>* kidneys compared with wild type at P20 (Figures 1b and c).

Time-course analysis revealed normal kidney histology at embryonic day (E) 18.5, with damage becoming evident by P3 and progressing in severity until death at ~P20 (Supplementary Figure 1). The lack of kidney pathology at E18.5 suggests that kidney development occurs normally in *Nedd4-2*-deficient mice.

**Generation of renal-tubule-specific *Nedd4-2*-deficient mice.** After identifying a critical new role for NEDD4-2 in renal homeostasis, we next aimed to investigate the progression of kidney injury beyond 20 days. To this end, we generated a renal-tubule-specific *Nedd4-2* KO mouse line by crossing a previously generated *Nedd4-2<sup>fl/fl</sup>* mouse line (with ablation of *Nedd4-2* exon 15 onward, resulting in the absence of the catalytic HECT domain and a complete loss of Nedd4-2 protein)<sup>10</sup> to the *Ksp1.3-Cre* transgene line.<sup>12</sup> *Ksp-cadherin*, also called *cadherin-16*, has a well-characterized, kidney-specific expression in renal epithelial cells of the collecting ducts, loop of Henle, the majority of proximal tubules and in some distal tubules.<sup>13</sup> Therefore, *Ksp1.3-Cre; Nedd4-2<sup>fl/fl</sup>* blocks NEDD4-2 expression in cadherin-16-positive cells and is hereafter referred to as *Nedd4-2<sup>Ksp1.3</sup>*. Immunoblot analysis of whole kidney lysates from this strain showed a decrease in NEDD4-2 protein compared with control kidneys (Cre negative) at P40 (Figure 2a). This was quantitated to an average reduction of ~50% (Figure 2b).

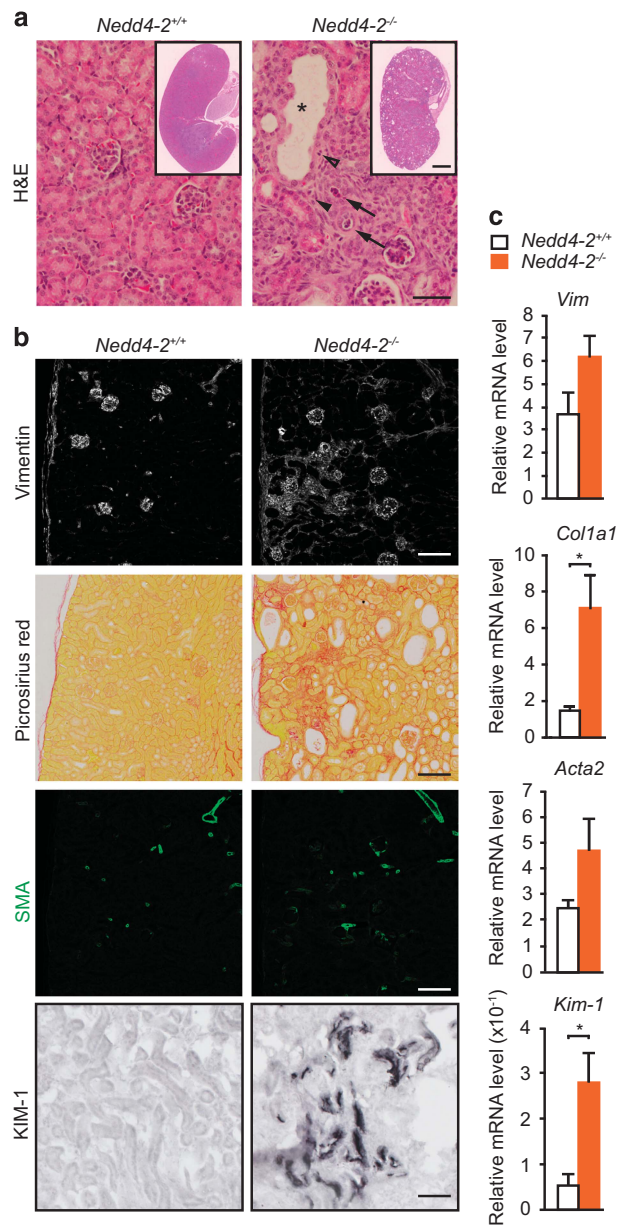


**Figure 1** Loss of NEDD4-2 results in kidney injury in juvenile mice. (a) Representative images showing hematoxylin–eosin (H&E) staining. Pathological observations include enlarged tubules (\*), cellular debris within tubules (arrows) and mesenchyme infiltration (arrowheads). (b) Immunostaining shows increased expression of vimentin (mesenchymal marker), (SMA; myofibroblasts) and KIM-1 (marker of proximal tubule kidney injury). Picosirius red staining demonstrates fibrosis in *Nedd4-2<sup>-/-</sup>* kidneys. (c) Increased gene expression for markers of kidney pathology, including collagen (encoded by *Col1a1*), vimentin (*Vim*), SMA (*Acta2*) and *Kim-1*, as determined by qRT-PCR in *Nedd4-2<sup>+/+</sup>* or *Nedd4-2<sup>-/-</sup>* mice. Data are normalized to *tbp* levels and represent mean  $\pm$  S.E.M. for four mice per genotype. \* $P < 0.05$ . Scale bars: (a) = 50  $\mu$ m, inset = 1 mm; (b) (vimentin, picosirius red and SMA) = 100  $\mu$ m, (KIM-1) = 50  $\mu$ m

Remaining NEDD4-2 is likely due to expression within the glomerulus, blood vessels and any other cells that do not express cadherin-16, but express NEDD4-2.<sup>12,13</sup> Immunohistochemical staining of control kidneys demonstrated high

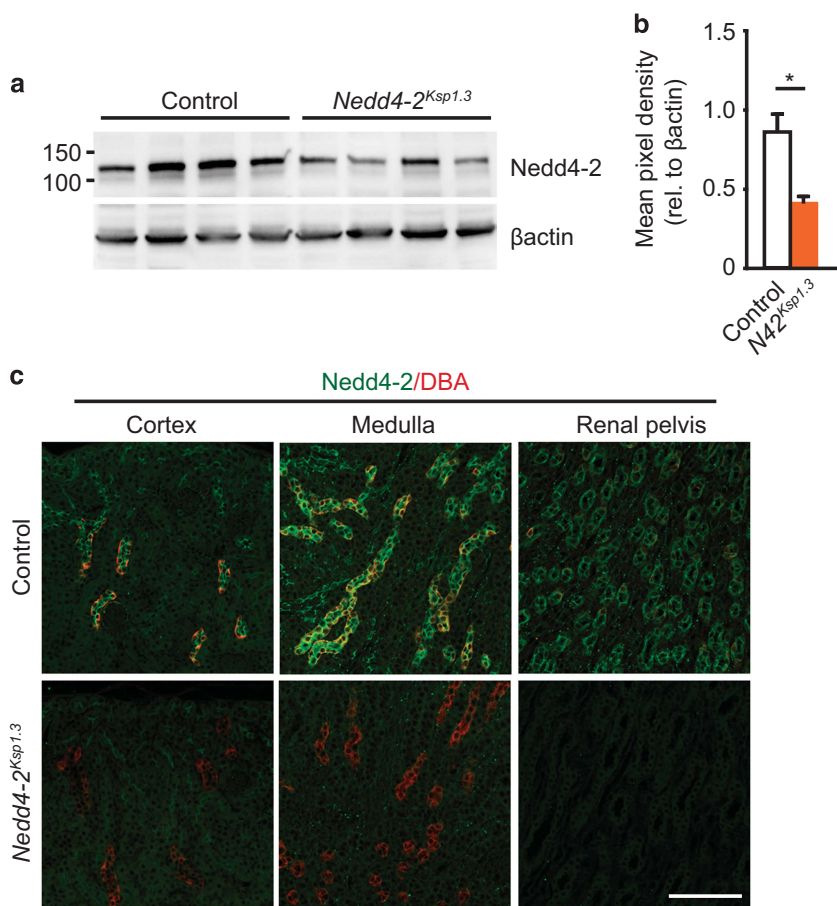


**Figure 2** Generation of the renal-tubule-specific *Nedd4-2* KO mice. (a) Semiquantitative immunoblot showing reduced NEDD4-2 expression in *Nedd4-2<sup>Ksp1.3</sup>* versus control mice at P40. Quantitated in (b) relative to  $\beta$ -actin expression to show an average reduction of ~50% with remaining NEDD4-2 likely due to expression within the renal corpuscle, blood vessels and any other cells that do not express cadherin-16 but express NEDD4-2.<sup>12,13</sup> (c) Immunohistochemical staining demonstrated high NEDD4-2 (green) expression within the distal nephron of control mice, including the collecting ducts as indicated by overlapping expression with the lectin marker, DBA (red). Importantly, NEDD4-2 expression was completely abolished in the distal renal tubule of *Nedd4-2<sup>Ksp1.3</sup>* kidneys. Scale bars: (c) = 50  $\mu$ m. \* $P < 0.05$

NEDD4-2 expression within the distal nephron including the collecting ducts, indicated by overlapping expression with the lectin marker, dolichos biflorus agglutinin (DBA) (Figure 2c). Importantly, NEDD4-2 expression was completely abolished in the distal renal tubule of *Nedd4-2<sup>Ksp1.3</sup>* kidneys.

***Nedd4-2* ablation in renal tubules leads to renal pathology.** *Nedd4-2<sup>Ksp1.3</sup>* revealed a similar progressive renal pathology to the global *Nedd4-2<sup>-/-</sup>* mice, with a slightly later onset. Macroscopic analysis revealed only minor differences between control and *Nedd4-2<sup>Ksp1.3</sup>* kidneys at P20 progressing to mild changes at P40 evident by an irregular border and small areas of disorganized tissue (Figure 3a). At 6 months, the kidneys appeared pale with small cysts in the cortex and a hydronephrotic renal pelvis. Histological staining showed increased tissue disorganization, tubule enlargement and fibrosis, starting from small isolated regions at P20 to larger fibrotic regions radiating in from the cortex at 6 months (Figure 3b). Closer analysis of *Nedd4-2<sup>Ksp1.3</sup>* mice at P40 showed enlarged tubules, with thinning or hypercellular epithelium, necrotic cellular debris and significant collagen deposition throughout the cortex and medulla as visualized

by picosirius red staining (Figures 4a and b). Consistent with this result, mRNA levels of *Col1a1* were higher in *Nedd4-2<sup>Ksp1.3</sup>* mice (Figures 4d). Similar to the *Nedd4-2<sup>-/-</sup>* mice, vimentin, SMA and KIM-1 expression were also increased demonstrating kidney injury (Figures 4c and d and Supplementary Figure 2). Immune cell infiltration was apparent in the *Nedd4-2<sup>Ksp1.3</sup>* kidney parenchyma, as seen by immunostaining for the T-lymphocyte marker, CD3 (Figures 4e and f).

Active caspase-3 staining was used to determine whether tubule epithelial cells were undergoing apoptosis. Figures 4g and h show a significant increase in the number of cleaved caspase-3-positive cells in *Nedd4-2<sup>Ksp1.3</sup>* kidneys compared with controls. Apoptotic cells were evident lining the tubules and also accumulating in the enlarged tubular lumens, detectable as early as P20 (Supplementary Figures 3a and b). In addition, some tubular epithelial cells also appeared swollen with enlarged nuclei, indicating necrotic changes to the lining epithelium in the absence of NEDD4-2 (Supplementary Figure 3c). Loss of tubule epithelial cells at an early age indicates that this may be an early manifestation of the renal disease.

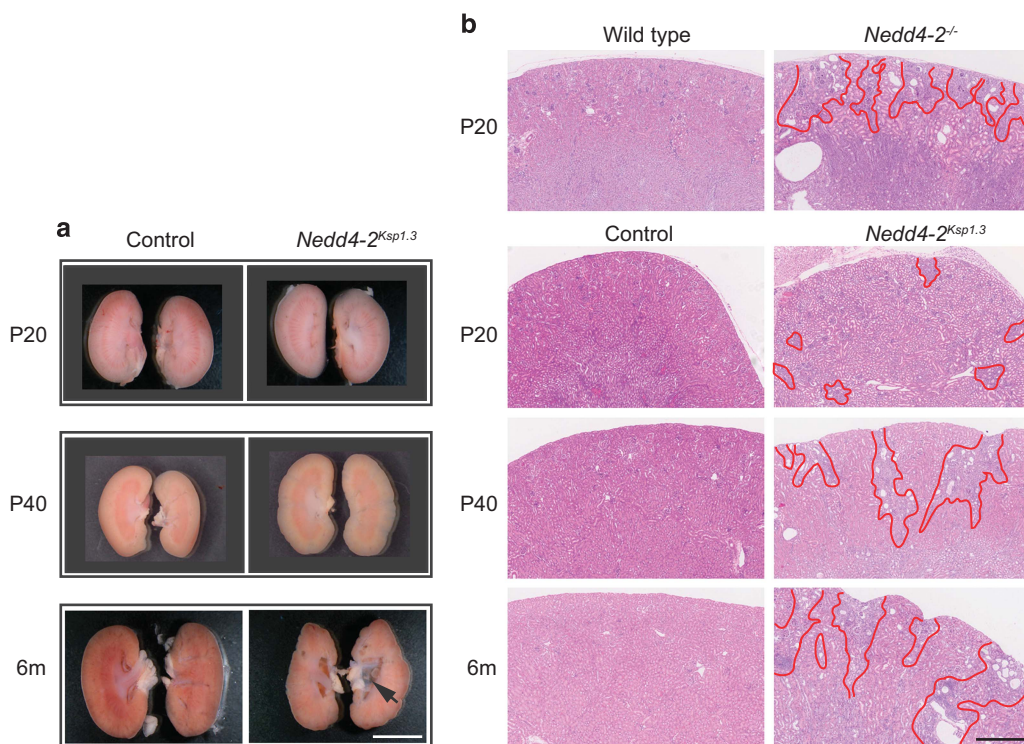


**Figure 3** Disease progression in *Nedd4-2<sup>Ksp1.3</sup>* mice compared with *Nedd4-2<sup>-/-</sup>* and control mice. (a) Macroscopic images of *Nedd4-2<sup>Ksp1.3</sup>* kidneys at P20, 40 and 6 months show disease progression. Indentations in the cortex are obvious at P40 and 6 months, and hydronephrosis develops only by 6 months (arrow). (b) Hematoxylin–eosin (H&E) shows regions of kidney damage in *Nedd4-2<sup>-/-</sup>* kidneys at P20, compared with time course of disease progression in *Nedd4-2<sup>Ksp1.3</sup>* kidneys (areas of damage are outlined in red). Scale bars: (a) = 5  $\mu\text{m}$  and (b) = 500  $\mu\text{m}$

**Nedd4-2 deficiency leads to increased expression of ENaC and NCC.** We next wanted to determine whether the levels of ENaC and NCC are altered in *Nedd4-2<sup>Ksp1.3</sup>* kidneys and could contribute to the renal disease observed in *Nedd4-2*-deficient animals. During the process of maturation, all three subunits of ENaC ( $\alpha$ ,  $\beta$  and  $\gamma$ ) are post-translationally modified. The  $\alpha$  and  $\gamma$  subunits are processed by proteolytic cleavage to their mature forms, and the  $\beta$ -subunit undergoes glycoprotein processing.<sup>14,15</sup> It is the mature ENaC complexes that are predominantly localized at the plasma membrane where they are regulated by NEDD4-2.<sup>16</sup> Immunostaining of *Nedd4-2<sup>Ksp1.3</sup>* kidneys at P40 demonstrated increased expression of all three ENaC subunits in the collecting ducts (Figures 5a). Semiquantitative analysis by immunoblot demonstrated upregulation of the mature forms of the ENaC subunits, and no change in the levels of the full-length, unprocessed forms, indicating that the loss of NEDD4-2 expression in renal tubules results in increased levels of mature ENaC at the plasma membrane (Figures 5b and c). Interestingly, cells with high ENaC expression could be seen lining dilated tubules and accumulating within the lumens (Figures 5d).

We next examined the levels of NCC in *Nedd4-2<sup>Ksp1.3</sup>* kidneys at P40. Immunostaining indicated higher levels of NCC protein in *Nedd4-2<sup>Ksp1.3</sup>* kidneys compared with control (Figures 5e and f). Immunoblot analysis of *Nedd4-2<sup>Ksp1.3</sup>* whole kidney lysates showed a similar increase in NCC expression (Figures 5g and h), confirming previous findings that NCC is regulated by NEDD4-2.<sup>4</sup>

**Increased BP and salt reabsorption in *Nedd4-2<sup>Ksp1.3</sup>* mice.** *Nedd4-2<sup>Ksp1.3</sup>* mice had increased blood  $\text{Na}^+$  concentration, reduced blood  $\text{K}^+$  concentration and increased  $\text{K}^+$  excretion on a standard laboratory diet (Table 1), which has not been previously observed in other *Nedd4-2* KO models, even on a high-salt diet.<sup>7,8</sup> *Nedd4-2<sup>Ksp1.3</sup>* mice also produced more urine with a significantly lower osmolarity than their control counterparts, possibly as a result of the increased  $\text{Na}^+$  reabsorption. Glomerular filtration rate (GFR) at 6 months was unchanged compared with controls. Importantly, diastolic (DBP) and systolic BP (SBP) were significantly higher in *Nedd4-2<sup>Ksp1.3</sup>* mice and blood aldosterone levels were reduced (Figure 6). Aldosterone has a central role in  $\text{Na}^+$  conservation in the body and is regulated by the blood serum levels of  $\text{K}^+$  and inversely by the levels of  $\text{Na}^+$ . Low aldosterone levels therefore indicate increased  $\text{Na}^+$ /reduced  $\text{K}^+$  retention in *Nedd4-2<sup>Ksp1.3</sup>* mice even on a normal laboratory diet. Taken together, these results demonstrate the critical role of NEDD4-2 in regulating  $\text{Na}^+$  and  $\text{K}^+$  levels in the blood.

**Kidney damage is reduced by inhibition of ENaC.** To determine if ENaC and NCC could give rise to the kidney damage, we treated mice with either amiloride (a specific inhibitor of ENaC) or hydrochlorothiazide (HCTZ; to block NCC) from P20 (weaning) until P41 (Figure 7a). Blood aldosterone was significantly increased upon treatment with amiloride in both controls and *Nedd4-2<sup>Ksp1.3</sup>* mice (Figure 7b), correlating with the expected effects of amiloride

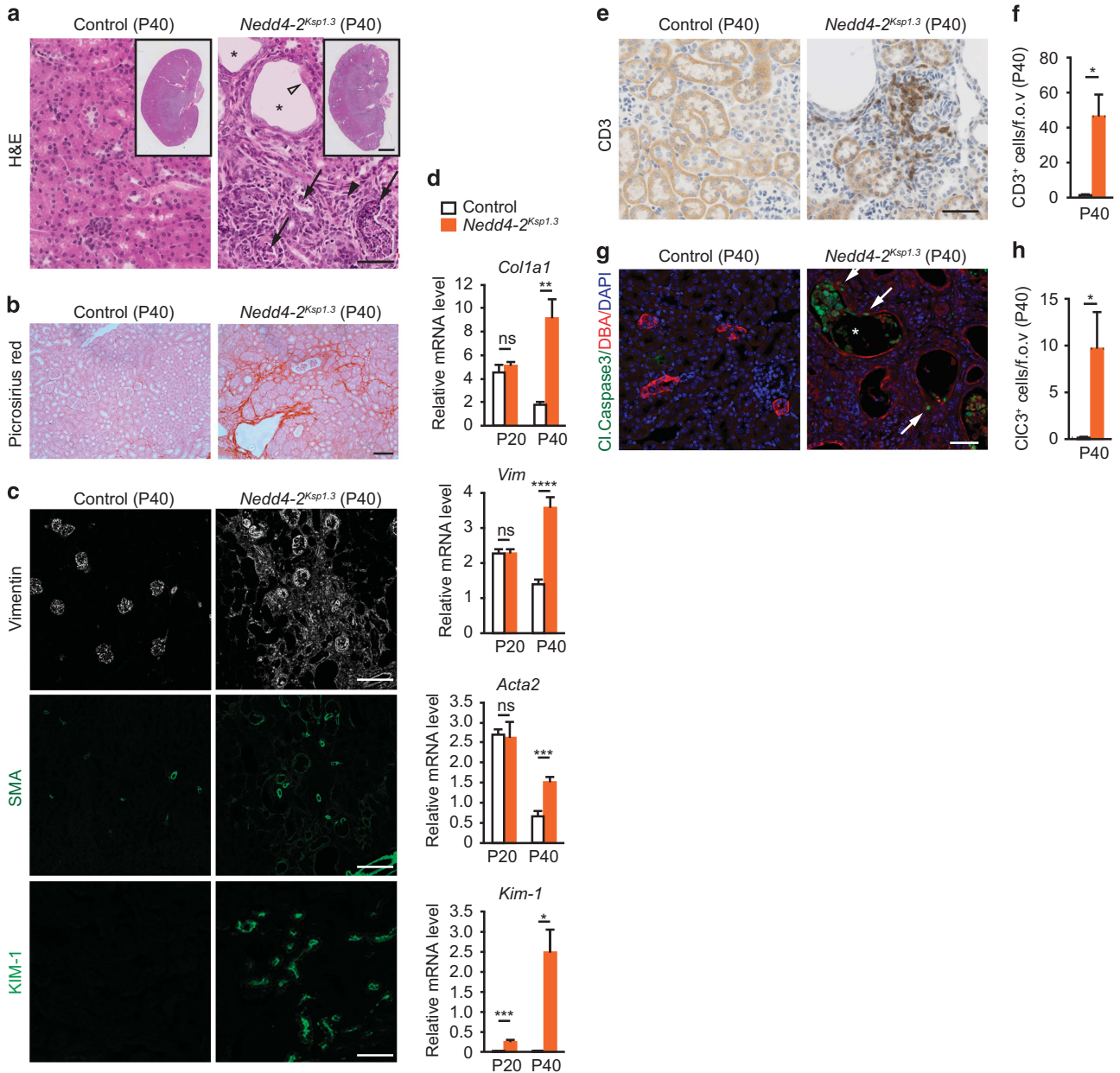


**Figure 4** Progressive kidney injury in kidney-specific *Nedd4-2* KO mice. (a) Representative hematoxylin–eosin (H&E) images show enlarged tubules (black asterisk), thinning of lining epithelium (open arrowhead), cellular debris within tubules (black arrows) and mesenchyme infiltration (black arrowhead) in P40 *Nedd4-2<sup>Ksp1.3</sup>* mice. (b) Picrosirius red staining demonstrates fibrosis in *Nedd4-2<sup>Ksp1.3</sup>* kidneys (red). (c) Immunostaining shows increased expression of vimentin, SMA and Kim-1. (d) Increased gene expression for markers of kidney injury at P40, including collagen (encoded by *Col1a1*), vimentin (*Vim*), SMA (*Acta2*) and *Kim-1*, determined by qRT-PCR. Only *Kim-1* levels were significantly altered at P20. Data are normalized to *tpb* levels and represent mean  $\pm$  s.e.m. for four mice per genotype. (e) Immune cell infiltration demonstrated by staining for CD3 (T-lymphocyte marker; and quantitated in (f)). (g and h) Immunostaining and quantitation of cleaved caspase-3-expressing cells shows apoptotic cells within tubules (white asterisk) and lining epithelia (white arrows) of *Nedd4-2<sup>Ksp1.3</sup>* kidneys at P40. (f and h)  $n = 4$  per genotype. \* $P < 0.05$ , \*\* $P < 0.01$ , \*\*\* $P < 0.005$  and \*\*\*\* $P < 0.001$ . Scale bars: (a) = 50  $\mu$ m, inset = 1 mm; (b) = 100  $\mu$ m; (c) vimentin and SMA = 100  $\mu$ m, Kim-1 = 50  $\mu$ m; (e and g) = 50  $\mu$ m. fov, Field of view; NS = not significant ( $P > 0.05$ )

to block ENaC-mediated  $\text{Na}^+$  reabsorption. In untreated *Nedd4-2<sup>Ksp1.3</sup>* kidneys, there was a significant increase in expression levels of *Vim* and *Kim-1* when compared with untreated controls, as detected by qRT-PCR (Figures 7c and d). Importantly, in *Nedd4-2<sup>Ksp1.3</sup>* P40 kidneys amiloride treatment reduced the expression of both *Vim* and *Kim-1*. These data suggest that inhibiting ENaC activity with amiloride was able to alleviate the disease phenotype. On

the contrary, HCTZ treatment had little beneficial effect in alleviating the kidney pathology. These results were supported by immunostaining for KIM-1 (Figures 7e and f). Taken together, these data demonstrate for the first time that a lack of NEDD4-2 increases  $\text{Na}^+$  reabsorption through increased expression and activity of ENaC, and that this results in kidney damage as well as hypertension on a standard laboratory diet.

**Discussion**

In this study, we have identified a novel link between *Nedd4-2* deficiency and nephropathy. We report for the first

time that deletion of *Nedd4-2* in the kidney results in a progressive kidney pathology characterized by renal fibrosis, cortical cysts, inflammation and tubular epithelial cell apoptosis. We have shown that this pathology critically involves

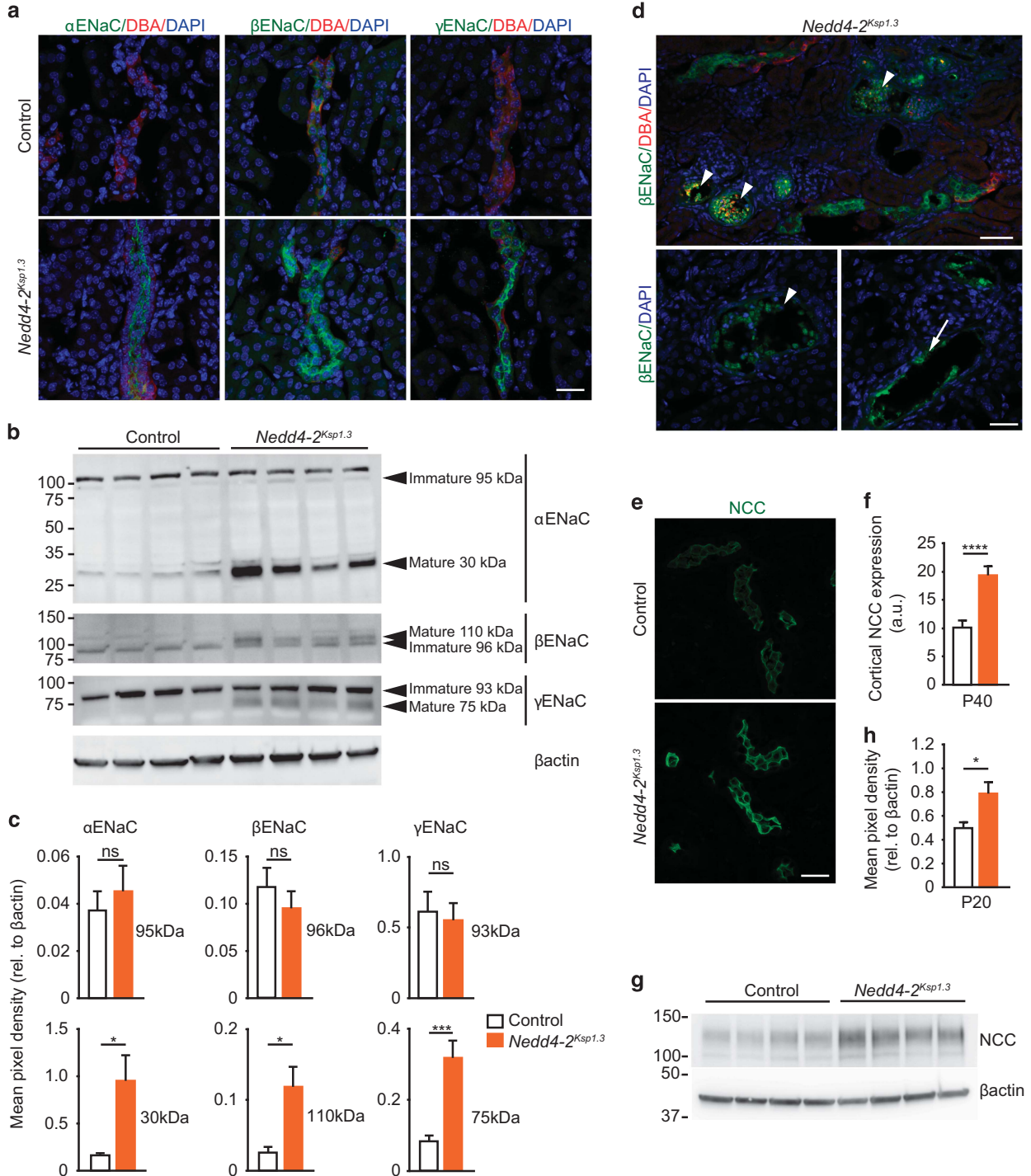


**Figure 5** Increased expression of active ENaC and NCC in P40 *Nedd4-2<sup>Ksp1.3</sup>* mice. (a) Representative images showing increased  $\alpha$ ,  $\beta$  and  $\gamma$  ENaC subunits in *Nedd4-2<sup>Ksp1.3</sup>* kidneys also demonstrated by western blot (b) and quantified in (c). Note that only the mature forms of each subunit (cleaved and/or post-translationally modified) are upregulated in *Nedd4-2<sup>Ksp1.3</sup>* mice. (d) Representative images show  $\beta$  ENaC (green) localized to the damaged epithelium (arrows) and cellular debris inside tubules (arrowheads) in *Nedd4-2<sup>Ksp1.3</sup>* kidneys. (e-h) NCC is upregulated in *Nedd4-2<sup>Ksp1.3</sup>* kidneys as shown by immunohistochemistry in (e), quantitated in (f), and by immunoblot analysis (g and h). Data are presented as mean  $\pm$  s.e.m. (f)  $n=3$  per genotype. \* $P<0.05$ , \*\* $P<0.01$  and \*\*\* $P<0.005$ . Scale bars: (a and e)=25  $\mu$ m (P40), (d) (top)=25  $\mu$ m, (bottom)=12.5  $\mu$ m (P40)

**Table 1** Urine and plasma electrolytes in control and tubule-specific *Nedd4-2<sup>Ksp1.3</sup>* mice at 6 months

	Control		<i>Nedd4-2<sup>Ksp1.3</sup></i>		P-value
Body weight (g)	33.838 ± 1.0192	[5]	27.22 ± 0.6788	[7]*	0.025
<i>Intake</i>					
Food (g/g BW/24h)	0.085 ± 0.007	[5]	0.182 ± 0.016	[7]*	0.013
Water (ml/g BW/24h)	0.164 ± 0.034	[5]	0.427 ± 0.113	[7]*	0.018
<i>Output</i>					
Feces (g/g BW/24 h)	0.023 ± 0.003	[5]	0.059 ± 0.008	[7]*	0.025
Urine (ml/g BW/24 h)	0.033 ± 0.005	[5]	0.241 ± 0.083	[7]*	0.025
Na <sup>+</sup> excretion (μmol/24 h)	124.824 ± 22.630	[5]	125.156 ± 26.725	[7]	0.631
Na <sup>+</sup> /Cr (10 <sup>3</sup> )	29.740 ± 2.517	[5]	29.664 ± 3.750	[7]	0.631
K <sup>+</sup> excretion (μmol/24h)	239.096 ± 28.534	[5]	359.383 ± 48.426	[7]	0.070
K <sup>+</sup> /Cr (10 <sup>3</sup> )	59.050 ± 5.659	[5]	87.204 ± 6.161	[7]*	0.010
Na <sup>+</sup> /K <sup>+</sup>	0.522 ± 0.063	[5]	0.339 ± 0.015	[7]*	0.030
Ca <sup>2+</sup> excretion (μmol/24h)	2.51635 ± 0.5	[3]	15.8835 ± 1.9629	[7]*	0.017
Ca <sup>2+</sup> /Cr (10 <sup>3</sup> )	0.61869 ± 0.0063	[3]	4.627573 ± 1.2878	[7]*	0.017
Urea excretion (μmol/24h)	1212.949 ± 169.696	[5]	1608.448 ± 202.021	[7]	0.260
Urea/Cr (10 <sup>3</sup> )	295.483 ± 26.187	[5]	389.929 ± 22.714	[7]*	0.048
Protein excretion (μg/24h)	3200.755 ± 666.685	[5]	2421.292 ± 388.522	[7]	0.429
Protein/Cr (10 <sup>3</sup> )	825.425 ± 157.029	[5]	608.037 ± 94.994	[7]	0.268
GFR (ml/g BW/24 h)	7.055 ± 1.108	[5]	7.371 ± 0.888	[7]	0.710
<i>Plasma</i>					
Na <sup>+</sup> (mM)	147.600 ± 0.454	[24]	152.600 ± 0.832	[16]***	< 0.0001
K <sup>+</sup> (mM)	3.736 ± 0.097	[24]	2.731 ± 0.131	[16]***	< 0.0001

Values are given as average ± s.e.m. Number of mice are indicated in square brackets. P-values were determined using a Mann-Whitney test for non-normally distributed data. \*P < 0.05, \*\*\*P < 0.005. Number of animals analyzed are shown within parentheses [n]

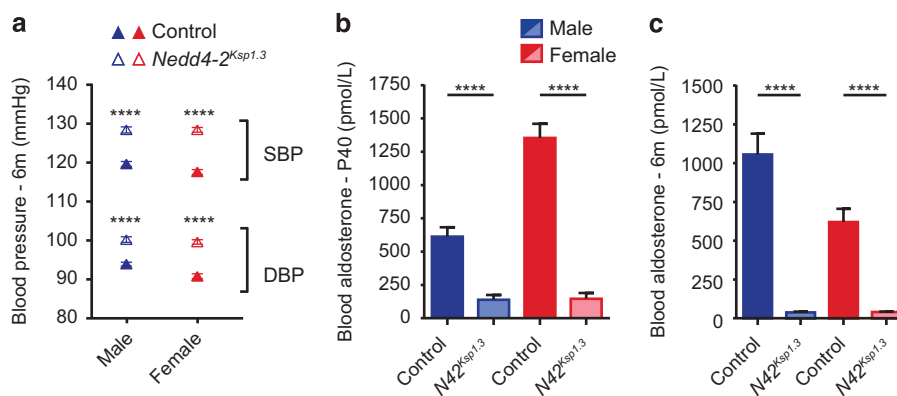


**Figure 6** *Nedd4-2<sup>Ksp1.3</sup>* mice have increased BP. (a) SBP and DBP of 6-month-old control and *Nedd4-2<sup>Ksp1.3</sup>* mice. (b and c) Blood serum aldosterone levels were significantly reduced in the *Nedd4-2<sup>Ksp1.3</sup>* mice as compared with the control mice at the age of P40 (b) and 6 months (c). All mice were fed a standard laboratory diet. BP was recorded from six to seven mice per genotype (control and *Nedd4-2<sup>Ksp1.3</sup>*) and gender. \*\*\*\*P < 0.001

regulation of salt uptake via ENaC, even on a standard laboratory diet.

**Absence of *Nedd4-2* results in kidney damage.** As described previously, most *Nedd4-2<sup>-/-</sup>* mice die perinatally from respiratory distress.<sup>5</sup> However, the few *Nedd4-2<sup>-/-</sup>* mice that survive display progressive kidney damage developing shortly after birth, with pathological features similar to those commonly observed in patients with nephropathies, such as fibrosis, cortical cysts, enlarged tubules and cellular casts.<sup>17</sup> Given the early postnatal lethality of *Nedd4-2<sup>-/-</sup>* mice, we generated a renal-tubule-specific line (*Nedd4-2<sup>Ksp1.3</sup>*) to investigate the cause of this kidney

damage. *Nedd4-2<sup>Ksp1.3</sup>* mice display a progressive renal pathology similar to the global *Nedd4-2<sup>-/-</sup>* mice, characterized by significant tubular epithelial cell apoptosis and fibrosis. By 6 months of age, *Nedd4-2<sup>Ksp1.3</sup>* mice develop prominent phenotypes of chronic kidney disease (CKD), including hydronephrosis, polyuria and polydipsia. *Nedd4-2<sup>Ksp1.3</sup>* mice display increased serum Na<sup>+</sup> levels and increased K<sup>+</sup> excretion, as well as high BP and low aldosterone, which are all indicative of increased Na<sup>+</sup> retention. Somewhat surprisingly *Nedd4-2<sup>Ksp1.3</sup>* mice maintained normal GFR at 6 months old, which is most likely due to remaining *Nedd4-2* expression in the glomerulus and the progressive nature of the disease.

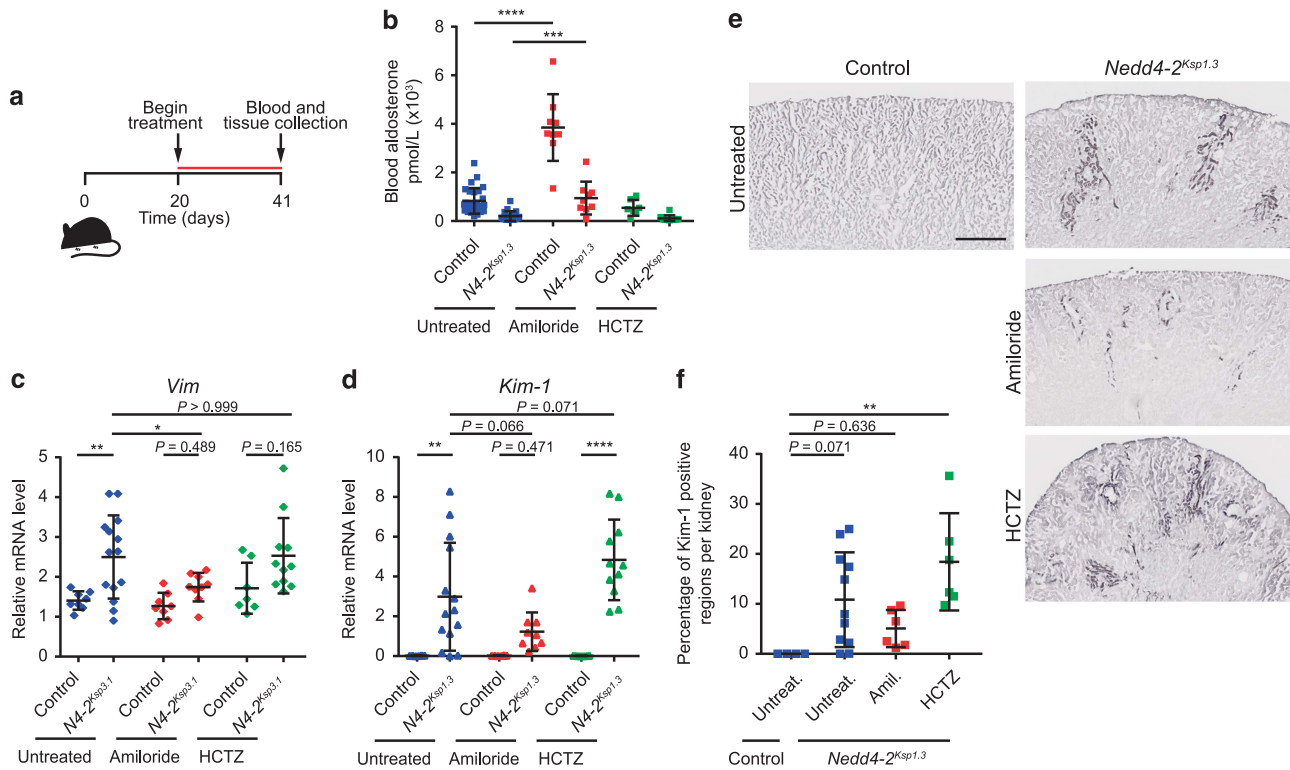


**Figure 7** Treatment of *Nedd4-2<sup>Ksp1.3</sup>* mice with diuretic drugs to block ENaC and NCC variably affects kidney damage. **(a)** Time course of treatment from P20 until P40. Drugs were added to the drinking water daily: amiloride (2 mg/kg) and HCTZ (10 mg/kg). **(b)** Blood aldosterone levels are shown for all treatment groups at P40. Amiloride treatment increases levels of aldosterone, as expected. **(c)** qRT-PCR data showing *Vimentin* and *Kim-1* expression levels in control and *Nedd4-2<sup>Ksp1.3</sup>* kidneys, administered with diuretic drugs in the tap water. **(e)** and **(f)** Representative images of *Kim-1* immunostaining showing areas of kidney damage in the cortex in untreated and treated mice **(e)**, and the result of quantitation **(f)**. **(b–d)**  $n = 9–14$ . **(f)** Samples were randomly selected from drug treatment experiment;  $n = 4–6$  for control untreated and *Nedd4-2<sup>Ksp1.3</sup>* amiloride and HCTZ treated,  $n = 11$  for *Nedd4-2<sup>Ksp1.3</sup>* untreated (one dot represents one mouse). \* $P < 0.05$ , \*\* $P < 0.01$ , \*\*\* $P < 0.005$  and \*\*\*\* $P < 0.001$ . Data are presented as mean  $\pm$  s.d. One-way analysis of variance (ANOVA) with Bonferroni’s post-test for comparison between multiple groups was used. Scale bar: **(e)** = 500  $\mu$ m

Hypertension is known to contribute to kidney damage and CKD.<sup>18</sup> In both *Nedd4-2<sup>-/-</sup>* and *Nedd4-2<sup>Ksp1.3</sup>* mice, kidney damage begins soon after birth indicating that this pathology is unlikely to be a secondary effect of hypertension. Furthermore, additional models of *Nedd4-2* deletion, which exhibit a similar degree of hypertension, display no evidence of kidney damage.<sup>7,8</sup> These data suggest that the kidney pathology observed in *Nedd4-2* KO mice is due to a primary effect on the tubular epithelia rather than as a result of hypertension.

**Kidney pathology caused by increased ENaC expression.** Importantly, our *Nedd4-2* KO mice develop kidney damage on a standard laboratory diet, and the increased  $\text{Na}^+$  reabsorption appears to be due, at least in part, to increased levels of ENaC on the plasma membrane. Indeed, we observed greater expression of the active forms of all three ENaC subunits in the collecting ducts of *Nedd4-2<sup>Ksp1.3</sup>* kidneys. In addition, we also observed a significant increase in levels of NCC, which was noted in the *Nedd4L<sup>Pax8/LC1</sup>* model.<sup>8</sup> The discrepancy in ENaC expression levels between different *Nedd4-2* mutant mouse models can be explained by some expression of functional *Nedd4-2* splice variants in other *Nedd4-2* mutant mouse lines.<sup>5</sup> In our *Nedd4-2<sup>Ksp1.3</sup>*

mice, no functional NEDD4-2 can be expressed given that the HECT domain is targeted.

The significance of increased levels of active ENaC in the development of kidney disease in *Nedd4-2<sup>Ksp1.3</sup>* mice is clear from our data showing that amiloride treatment reduces renal damage. Thus, increased functional ENaC at the plasma membrane appears to be a contributing factor to the development of kidney disease. Indeed, ENaC has been implicated in the development of kidney damage in Dahl salt-sensitive rats that develop hypertension and renal damage after 4 weeks on a high-salt diet.<sup>19,20</sup>

In our *Nedd4-2<sup>Ksp1.3</sup>* mice, inhibition of NCC alone (with HCTZ) was not able to rescue the disease phenotype in our *Nedd4-2<sup>Ksp1.3</sup>* mice, suggesting that ENaC, and not NCC, is a major contributor to the disease. Administration of amiloride, however, did not fully rescue the kidney damage seen in *Nedd4-2<sup>Ksp1.3</sup>* mice. We therefore hypothesize that in addition to increased  $\text{Na}^+$  absorption by ENaC, other NEDD4-2-regulated mechanisms may contribute to the renal pathology seen in *Nedd4-2*-deficient animals.

**Clinical significance of NEDD4-2 in salt induced kidney damage.** The effect of *Nedd4-2* deficiency in renal pathology has not been previously characterized. There is



evidence that *Nedd4-2* contributes to salt-sensitive hypertension in humans, as multiple single-nucleotide polymorphisms (SNPs) in this gene have been linked to increased ENaC expression and hypertension.<sup>21–25</sup> However, their possible role in kidney disease has not been reported. In a previous study assessing NEDD4L variants in hypertension, two patients with a nonsynonymous variant of *NEDD4L* were also found to have end-stage renal disease (ESRD).<sup>26</sup> Thus, SNPs of *NEDD4L* can lead to hypertension, as well as contribute to renal diseases in patients, similar to that observed in the *Nedd4-2*<sup>-/-</sup> and *Nedd4-2*<sup>Ksp1.3</sup> mice.

## Conclusions

Approximately 1 in 10 people worldwide suffer from varying degrees of CKD, and those with hypertension or diabetes are at even higher risk.<sup>27</sup> In addition, CKD can itself contribute to hypertension and cardiovascular disease further fueling the burden of CKD on healthcare systems worldwide.<sup>28</sup> Acute kidney injury can initiate the onset of chronic and ESRD<sup>29,30</sup> and is therefore an important focus for early intervention to limit kidney pathology. NEDD4-2 is a critical regulator of Na<sup>+</sup> ion channels along the nephron, and polymorphisms in the human *NEDD4L* gene are associated with salt-sensitive hypertension and kidney disease. This makes NEDD4-2, and proteins that may regulate it, important targets for the development of therapeutics for improved health care of patients with kidney disease. The studies reported here provide new data toward the understanding of the function of NEDD4-2, its critical role in Na<sup>+</sup> homeostasis, and the contribution of increased Na<sup>+</sup> reabsorption to renal disease.

## Materials and Methods

**Mouse lines.** Global *Nedd4-2*<sup>-/-</sup> mice were generated in our laboratory previously.<sup>5</sup> Kidney-specific inactivation of *Nedd4-2* was achieved by crossing the *Nedd4-2*-floxed line (*Nedd4-2*<sup>fl/fl</sup>)<sup>10</sup> with the Ksp-Cre transgenic strain from Peter Igarashi's laboratory (obtained through Christina Mitchell).<sup>12</sup> Homozygous *Nedd4-2*-floxed mice (*Nedd4-2*<sup>fl/fl</sup>) were crossed with heterozygous mice expressing the Ksp1.3-Cre transgene. From the filial (F) 1 progeny, litters with heterozygous deletion of *Nedd4-2* gene that harbored the Ksp1.3-Cre transgene (*Ksp1.3-Cre; Nedd4-2*<sup>fl/+</sup>) were selected and further crossed with *Nedd4-2*<sup>fl/fl</sup> mice to obtain mice expressing complete deletion of *Nedd4-2* in the F2 progeny (*Ksp1.3-Cre; Nedd4-2*<sup>fl/fl</sup>), referred to as *Nedd4-2*<sup>Ksp1.3</sup> mice. *Nedd4-2*<sup>-/-</sup> (C57BL/6 J) and *Nedd4-2*<sup>Ksp1.3</sup> (C57BL/6 J) mice were bred at the SA Pathology Animal Facility (Adelaide, Australia) under specific pathogen-free conditions. All animal studies were approved by the institutional animal ethics and biosafety committees at SA Pathology, and were carried out according to the National Health and Medical Research Council guidelines.

For tissue collection, mice were anesthetized and blood collected by cardiac puncture. Animals were then quickly killed by cervical dislocation. Kidneys were removed and the fibrous capsule dissected off. One kidney was snap frozen in liquid nitrogen, and the other was cut in half in the coronal plane and immersion fixed in Histochoice (ProSciTech, Kirwan, QLD, Australia) for 48 h at 4 °C. One-half of the kidney was paraffin embedded and the other half was embedded in OCT for frozen sections.

**Drug treatment studies.** For drug treatment studies, mice were treated with amiloride (Sigma-Aldrich, St. Louis, MO, USA; 2 mg/kg per day; 14 mg/l)<sup>31</sup> or HCTZ (Sigma-Aldrich; 10 mg/kg per day; 67 mg/l)<sup>32</sup> in the drinking water. Treatment began after weaning at P20, with water changed daily for 21 days. Animals were anesthetized for blood and tissue collection as above. During treatment, mice were group housed in standard conditions with free access to food and water and monitored daily.

**Metabolic cage studies.** Male, 6-month-old *Nedd4-2*<sup>Ksp1.3</sup> and control littermates were housed in metabolic cages for 24 h following three training sessions of 6 h each. Mice were provided *ad libitum* access to deionized drinking water and standard pelleted chow, and urine was collected every 5 h. At the end of the experiment, blood and tissue samples were taken as described above.

**Histological analysis.** Kidney tissues fixed in histochoice were embedded in paraffin and 5- $\mu$ m sections were cut using a paraffin microtome. The sections were mounted on glass slides, deparaffinized with xylene, dehydrated through graded series of ethanol and stained with hematoxylin–eosin. To evaluate collagen deposition using picrosirius red, slides were stained for 1 h in saturated picric acid with 0.1% Direct Red 80 (Sigma-Aldrich), and then washed in 0.01 N hydrochloric acid for 2 min. Digital images were acquired by using a NanoZoomer Imager (Hamamatsu Photonics K. K., Japan).

**Antibodies and immunohistochemistry.** Paraffin sections (5  $\mu$ m) were deparaffinized and hydrated in a graded ethanol series. Heat-mediated antigen retrieval was carried out by boiling for 10 min in 10 mM citric acid solution (pH 6). Tissue sections were blocked with 10% goat serum. Primary antibodies used were: rabbit anti- $\alpha$ ENaC and rabbit anti- $\gamma$ ENaC;<sup>33</sup> rabbit anti- $\beta$ ENaC;<sup>5</sup> fluorescein-conjugated Lotus tetragonolobus agglutinin (cat. no. FL-1321; Vector Laboratories, Burlingame, CA, USA); rhodamine-labeled DBA (cat. no. RL-1032; Vector Laboratories); FITC-conjugated mouse anti-SMA (cat. no. F3777; Sigma-Aldrich); rabbit anti-vimentin (cat. no. ab92547; Abcam, Cambridge, UK); rabbit anti-NCC (cat. no. ab3553; Abcam); rabbit anti-cleaved caspase-3 (cat. no. 9661 S; Cell Signaling Technologies, Danvers, MA, USA); rat anti-Kim-1 (cat. no. MAB1817; R&D Systems, Minneapolis, MN, USA). Immunostainings for Kim-1 and all ENaC subunits were carried out on frozen sections (14  $\mu$ m). For colorimetric staining, endogenous peroxidase was blocked by incubation in 3% hydrogen peroxide before primary antibody addition, sections were incubated with the corresponding biotinylated secondary antibodies and sequentially incubated in ABC-Peroxidase Solution according to the manufacturer's protocol (Thermo Fisher Scientific, Waltham, MA, USA), before being developed with 3,3'-diaminobenzidine (DAB; Sigma-Aldrich). Sections were lightly counterstained with hematoxylin, and then dehydrated and mounted. For fluorescence staining, tissue sections were incubated with the corresponding fluorescently tagged secondary antibodies (AlexaFluor-488 or -568; Thermo Fisher Scientific), counterstained with DAPI and mounted in Prolong Gold Antifade reagent (Thermo Fisher Scientific). Stained samples were imaged using an LSM 700 confocal microscope using Zen 2011 (Black Edition) version 8.1.5.484 (Carl Zeiss Microscopy, Jena, Germany) or NanoZoomer Imager (Hamamatsu Photonics K. K., Japan). Image analysis was carried out using ImageJ (NIH, Bethesda, MD, USA), Photoshop and Adobe Image Suite (Adobe, San Jose, CA, USA) Software.

**Quantification.** Cleaved caspase-3-positive or CD3-positive cells were counted in eight random cortical fields from four kidneys of each genotype at x20 magnification. Quantitation of total fluorescence from NCC-positive cells was carried out from 4–6 random fields in the cortex of three mice each for control and *Nedd4-2*<sup>Ksp1.3</sup> kidneys at x100 magnification. Total fluorescence levels for each image was measured using ImageJ (NIH). Percentage area of Kim-1-positive staining was measured in the cortex and medulla of drug-treated and -untreated mice. Frozen sections (14  $\mu$ m) from at least six mice per group were immunostained for Kim-1 and then developed using DAB. Each section was then imaged on the NanoZoomer Imager and the percentage area of Kim-1 staining in the cortex and medulla was quantitated using ImageJ (NIH).

**Immunoblotting.** Kidneys were lysed in ice-cold extraction buffer at pH 7.5 (50 mM Tris-HCl, pH 7.5, 1 mM EDTA, 1 mM EGTA, 0.27 M sucrose, 0.1%  $\beta$ -mercaptoethanol and HALT protease and phosphatase inhibitor cocktail; Thermo Fisher Scientific). Tissue was homogenized, frozen in liquid nitrogen, immediately thawed and incubated at 4 °C on a nutator for 30 min and centrifuged at 13 000 r.p.m. for 5 min. Supernatant protein (100  $\mu$ g) was combined with protein load buffer (100 mM Tris-HCl, pH 6.8, 200 mM DTT, 4% SDS, 0.2% bromophenol blue, 20% glycerol), heated at 95 °C for 5 min, loaded onto 4–20% precast SDS-PAGE gels (Bio-Rad, Hercules, CA, USA) and transferred to PVDF membrane using the Trans-Blot Turbo Instrument (Bio-Rad). Membranes were blocked with 1% skim milk in TBS-T (Tris-buffered saline/0.05% Tween-20) and primary antibodies were added: rabbit anti-Nedd4-2,<sup>34</sup> mouse anti- $\beta$ -actin (clone AC15; Sigma-Aldrich), or ENaC and NCC antibodies described above. HRP secondary antibodies were added

(Merck Millipore, Billerica, MA, USA) and developed with a ECL Prime substrate (GE Healthcare, Paramatta, NSW, Australia) on a ChemiDoc Touch Imager (Bio-Rad).

**Real-time quantitative PCR.** Total RNA was isolated from kidneys using TRIzol Reagent (Thermo Fisher Scientific) and RNA was reverse-transcribed with a High Capacity cDNA Reverse Transcription Kit (Applied Biosciences, Foster city, CA, USA). qRT-PCR was performed and analyzed as described,<sup>35</sup> where all data are normalized to *tbp* (TATA box-binding protein) levels. Primer sequences are detailed in Supplementary Table 1.

**BP measurements.** BP was measured by a tail cuff system (CODA Monitor; Kent Scientific Corporation, Torrington, CT, USA) as described previously.<sup>36</sup> Briefly, 6-month-old mice were placed into a plastic tube restrainer, BP recording cuffs were placed over the tail and the mice were allowed to adapt to the restrainer for 5 min. BP was then measured for 10 acclimation cycles followed by 25–30 measurement cycles. Heating pads were used to keep the mice warm throughout the experiment to ensure sufficient blood flow to the tail. Blood pressure was recorded from six to seven mice per genotype (control and *Nedd4-2*<sup>Ksp1.3</sup>) and gender.

**Electrolytes and aldosterone.** Electrolytes and aldosterone levels in blood and urine were carried out by SA Pathology. Urinary and plasma Na<sup>+</sup>, K<sup>+</sup>, Cl<sup>-</sup> and creatinine were measured using an Advia 2400 Chemistry System (Siemens, Bayswater, VIC, Australia), and urine osmolality was measured with an Advanced 3320 Osmometer (Advanced Instruments, Thermo Fisher Scientific, Waltham, MA, USA). Plasma aldosterone levels were measured using a Liaison Aldosterone Kit and a Chemiluminescent Analyzer (Diasorin, Saluggia, Italy). GFR was estimated based on creatinine clearance using a standard formula: GFR = urine flow x [urine creatinine]/[plasma creatinine].<sup>37</sup>

**Statistical analysis of data.** Statistical analysis was performed using GraphPad Prism software, version 6.0 (San Diego, CA, USA). One-way ANOVA with Bonferroni's post-test was used to assess rescue of kidney injury by qRT-PCR after treatment with diuretics in control and *Nedd4-2*<sup>Ksp1.3</sup> mice. Metabolic cage data and cleaved caspase-3 quantitation was assessed using a Mann–Whitney test for non-normally distributed data. Remaining data were analyzed using unpaired two-tailed Student's *t*-test with Welch's correction, *Nedd4-2*<sup>Ksp1.3</sup> versus controls. A *P*-value of ≤ 0.05 was considered significant. All values are presented as mean ± s.e.m. unless otherwise stated.

**Study approval.** All experimental procedures were approved by the SA Pathology/CALHN animal ethics committee and carried out in accordance with the local animal welfare act.

### Conflict of Interest

The authors declare no conflict of interest.

**Acknowledgements.** We are grateful to John Finnie for helping with the pathological analysis of kidneys, Ian Smyth and Darren Saunders for helpful discussions, Johannes Loffing for the gift of  $\alpha$  and  $\gamma$  ENaC antibodies, and Christina Mitchell for supplying the *Ksp1.3-Cre* mice following permission from Peter Igarashi. We also acknowledge the help of SA pathology animal house staff. This work was supported by a National Health and Medical Research Council (NHMRC) of Australia Senior Principal Research Fellowship (GNT1103006) and project grants (GNT1020755 and GNT1099307) to SK, and a Mary Overton Early Career Fellowship to JAM.

### Author contributions

JM, NAB and SK conceptualized the project; JM made the initial observation of renal pathology in *Nedd4-2*<sup>-/-</sup> animals; JM, OA, NAB and PG carried out early studies on characterization of the renal phenotype in *Nedd4-2*<sup>-/-</sup> animals; OA and NAB generated the *Nedd4-2*<sup>Ksp1.3</sup> mice and made initial observations on animal viability; TH and JM, with assistance from OA, carried out detailed pathophysiological analysis of *Nedd4-2*<sup>Ksp1.3</sup> and *Nedd4-2*<sup>-/-</sup> mice and performed the drug treatment experiments; TLH, JM, NAB, OA, PG and SK analyzed data; TLH, JAM and SK wrote the manuscript and HK provided the *Nedd4-2*<sup>oxP</sup> mice. All authors commented on the manuscript.

1. Harvey KF, Dinudom A, Cook DI, Kumar S. The Nedd4-like protein KIAA0439 is a potential regulator of the epithelial sodium channel. *J Biol Chem* 2001; **276**: 8597–8601.
2. Kamynina E, Debonneville C, Bens M, Vandewalle A, Staub O. A novel mouse Nedd4 protein suppresses the activity of the epithelial Na<sup>+</sup> channel. *FASEB J* 2001; **15**: 204–214.
3. Folia AB, Dinudom A, Shearwin KE, Koch JP, Korbmacher C, Cook DI et al. The role of individual Nedd4-2 (KIAA0439) WW domains in binding and regulating epithelial sodium channels. *FASEB J* 2003; **17**: 70–72.
4. Arroyo JP, Lagnaz D, Ronzaud C, Vazquez N, Ko BS, Moddes L et al. Nedd4-2 modulates renal Na<sup>+</sup>-Cl<sup>-</sup> cotransporter via the aldosterone-SGK1-Nedd4-2 pathway. *J Am Soc Nephrol* 2011; **22**: 1707–1719.
5. Boase NA, Rychkov GY, Townley SL, Dinudom A, Candi E, Voss AK et al. Respiratory distress and perinatal lethality in Nedd4-2-deficient mice. *Nat Commun* 2011; **2**: 287.
6. Araki N, Umemura M, Miyagi Y, Yabana M, Miki Y, Tamura K et al. Expression, transcription, and possible antagonistic interaction of the human Nedd4L gene variant: implications for essential hypertension. *Hypertension* 2008; **51**: 773–777.
7. Shi PP, Cao XR, Sweezer EM, Kinney TS, Williams NR, Husted RF et al. Salt-sensitive hypertension and cardiac hypertrophy in mice deficient in the ubiquitin ligase Nedd4-2. *Am J Physiol Renal Physiol* 2008; **295**: F462–F470.
8. Ronzaud C, Loffing-Cueni D, Hausel P, Debonneville A, Malsure SR, Fowler-Jaeger N et al. Renal tubular NEDD4-2 deficiency causes NCC-mediated salt-dependent hypertension. *J Clin Invest* 2013; **123**: 657–665.
9. Al-Qusairi L, Basquin D, Roy A, Rajaram RD, Maillard MP, Subramanya AR et al. Renal tubular ubiquitin-protein ligase NEDD4-2 is required for renal adaptation during long-term potassium depletion. *J Am Soc Nephrol* 2017; **28**: 2431–2442.
10. Kimura T, Kawabe H, Jiang C, Zhang W, Xiang YY, Lu C et al. Deletion of the ubiquitin ligase Nedd4L in lung epithelia causes cystic fibrosis-like disease. *Proc Natl Acad Sci USA* 2011; **108**: 3216–3221.
11. Ichimura T, Bonventre JV, Bailly V, Wei H, Hession CA, Cate RL et al. Kidney injury molecule-1 (KIM-1), a putative epithelial cell adhesion molecule containing a novel immunoglobulin domain, is up-regulated in renal cells after injury. *J Biol Chem* 1998; **273**: 4135–4142.
12. Shao X, Somlo S, Igarashi P. Epithelial-specific *Cre/lox* recombination in the developing kidney and genitourinary tract. *J Am Soc Nephrol* 2002; **13**: 1837–1846.
13. Grande MT, Sanchez-Laorden B, Lopez-Blau C, De Frutos CA, Boutet A, Arevalo M et al. Snail1-induced partial epithelial-to-mesenchymal transition drives renal fibrosis in mice and can be targeted to reverse established disease. *Nat Med* 2015; **21**: 989–997.
14. Hughey RP, Mueller GM, Bruns JB, Kinlough CL, Poland PA, Harkleroad KL et al. Maturation of the epithelial Na<sup>+</sup> channel involves proteolytic processing of the alpha- and gamma-subunits. *J Biol Chem* 2003; **278**: 37073–37082.
15. Ergonul Z, Frindt G, Palmer LG. Regulation of maturation and processing of ENaC subunits in the rat kidney. *Am J Physiol Renal Physiol* 2006; **291**: F683–F693.
16. Zhou R, Patel SV, Snyder PM. Nedd4-2 catalyzes ubiquitination and degradation of cell surface ENaC. *J Biol Chem* 2007; **282**: 20207–20212.
17. Wolf MT. Nephronophthisis and related syndromes. *Curr Opin Pediatr* 2015; **27**: 201–211.
18. Gargiulo R, Suhaif F, Lerma EV. Hypertension and chronic kidney disease. *Dis Mon* 2015; **61**: 387–395.
19. Kakizoe Y, Kitamura K, Ko T, Wakida N, Maekawa A, Miyoshi T et al. Aberrant ENaC activation in Dahl salt-sensitive rats. *J Hypertens* 2009; **27**: 1679–1689.
20. Pavlov TS, Levchenko V, O'Connor PM, Ilatovskaya DV, Palygin O, Mori T et al. Deficiency of renal cortical EGF increases ENaC activity and contributes to salt-sensitive hypertension. *J Am Soc Nephrol* 2013; **24**: 1053–1062.
21. Rizzo F, Staub O. NEDD4-2 and salt-sensitive hypertension. *Curr Opin Nephrol Hypertens* 2015; **24**: 111–116.
22. Dahlberg J, Nilsson LO, von Wowern F, Melander O. Polymorphism in NEDD4L is associated with increased salt sensitivity, reduced levels of P-renin and increased levels of Nt-proANP. *PLoS ONE* 2007; **2**: e432.
23. Russo CJ, Melista E, Cui J, DeStefano AL, Bakris GL, Manolis AJ et al. Association of NEDD4L ubiquitin ligase with essential hypertension. *Hypertension* 2005; **46**: 488–491.
24. Svensson-Farbom P, Wahlstrand B, Almgren P, Dahlberg J, Fava C, Kjeldsen S et al. A functional variant of the NEDD4L gene is associated with beneficial treatment response with beta-blockers and diuretics in hypertensive patients. *J Hypertens* 2011; **29**: 388–395.
25. McDonough CW, Burbage SE, Duarte JD, Gong Y, Langae TY, Turner ST et al. Association of variants in NEDD4L with blood pressure response and adverse cardiovascular outcomes in hypertensive patients treated with thiazide diuretics. *J Hypertens* 2013; **31**: 698–704.
26. Fouladkou F, Alikhani-Koopaei R, Vogt B, Flores SY, Malbert-Colas L, Lecomte MC et al. A naturally occurring human Nedd4-2 variant displays impaired ENaC regulation in *Xenopus laevis* oocytes. *Am J Physiol Renal Physiol* 2004; **287**: F550–F561.
27. Hill NR, Fatoba ST, Oke JL, Hirst JA, O'Callaghan CA, Lasserson DS et al. Global Prevalence of chronic kidney disease—a systematic review and meta-analysis. *PLoS ONE* 2016; **11**: e0158765.
28. National Kidney F. K/DOQI clinical practice guidelines for chronic kidney disease: evaluation, classification, and stratification. *Am J Kidney Dis* 2002; **39**(Suppl 1): S1–S266.

29. Zager RA, Johnson AC, Andress D, Becker K. Progressive endothelin-1 gene activation initiates chronic/end-stage renal disease following experimental ischemic/reperfusion injury. *Kidney Int* 2013; **84**: 703–712.
30. Zoja C, Abbate M, Remuzzi G. Progression of renal injury toward interstitial inflammation and glomerular sclerosis is dependent on abnormal protein filtration. *Nephrol Dial Transplant* 2015; **30**: 706–712.
31. Guo DF, Chenier I, Lavoie JL, Chan JS, Hamet P, Tremblay J *et al*. Development of hypertension and kidney hypertrophy in transgenic mice overexpressing ARAP1 gene in the kidney. *Hypertension* 2006; **48**: 453–459.
32. Reungjui S, Hu H, Mu W, Roncal CA, Croker BP, Patel JM *et al*. Thiazide-induced subtle renal injury not observed in states of equivalent hypokalemia. *Kidney Int* 2007; **72**: 1483–1492.
33. Rubera I, Loffing J, Palmer LG, Frindt G, Fowler-Jaeger N, Sauter D *et al*. Collecting duct-specific gene inactivation of alphaENaC in the mouse kidney does not impair sodium and potassium balance. *J Clin Invest* 2003; **112**: 554–565.
34. Konstas AA, Shearwin-Whyatt LM, Fotia AB, Degger B, Riccardi D, Cook DI *et al*. Regulation of the epithelial sodium channel by N4WBP5A, a novel Nedd4/Nedd4-2-interacting protein. *J Biol Chem* 2002; **277**: 29406–29416.
35. Foot NJ, Gembus KM, Mackenzie K, Kumar S. Ndfip2 is a potential regulator of the iron transporter DMT1 in the liver. *Sci Rep* 2016; **6**: 24045.
36. Feng M, Deerhake ME, Keating R, Thaisz J, Xu L, Tsaih SW *et al*. Genetic analysis of blood pressure in 8 mouse intercross populations. *Hypertension* 2009; **54**: 802–809.
37. Ronzaud C, Loffing J, Bleich M, Gretz N, Grone HJ, Schutz G *et al*. Impairment of sodium balance in mice deficient in renal principal cell mineralocorticoid receptor. *J Am Soc Nephrol* 2007; **18**: 1679–1687.



This work is licensed under a Creative Commons Attribution-NonCommercial-NoDerivs 4.0 International License. The images or other third party material in this article are included in the article's Creative Commons license, unless indicated otherwise in the credit line; if the material is not included under the Creative Commons license, users will need to obtain permission from the license holder to reproduce the material. To view a copy of this license, visit <http://creativecommons.org/licenses/by-nc-nd/4.0/>

© The Author(s) 2017

Supplementary Information accompanies this paper on Cell Death and Differentiation website (<http://www.nature.com/cdd>)